Effective SNR improvement using a high-power pulsed pump in an ytterbium-doped fiber amplifier

Jing Liu (刘 静), Lixin Xu (许立新)*, Anting Wang (王安廷), Chun Gu (顾 春), Qing Liu (刘 庆), Ankun Wei (魏安琨), Teng Xu (徐 腾), and Hai Ming (明 海)

Anhui Key Laboratory of Optoelectronic Science and Technology, Department of Optics and Optical Engineering, University of Science and Technology of China, Hefei 230026, China

**Corresponding author: xulixin@ustc.edu.cn*

Received May 4, 2013; accepted July 12, 2013; posted online August 30, 2013

A high-power pulsed pump method is proposed to obtain a high-energy output with an improved signal-to-noise ratio (SNR) during pulse amplification. Based on numerical analysis, the ytterbium-doped fiber amplifiers are compared under different pumping conditions. At the same signal gain, the output using the high-power pulsed pump shows great SNR improvement and reduced output signal distortion, compared with a continuous-wave pump and a low-power pulsed pump. By adjusting the pump parameters, the amplifier can achieve the optimal output SNR without sacrificing the signal gain. We believe that the high-power pulsed pump scheme is very suitable for the high-energy nanosecond pulse amplification, which has a high SNR requirement.

OCIS codes: 060.2320, 140.4480.
doi: 10.3788/COL201311.090603.

Fiber-based high-energy nanosecond pulses are highly desired in many applications, such as remote sensing, lidar, laser trimming, and material processing. These pulses are effectively generated by master oscillator power amplifier (MOPA) systems, wherein ytterbium-doped fiber amplifiers (YDFAs) are usually adopted[1]. The repetition rate of fiber amplifiers should be decreased to guarantee energy storage and achieve a high energy output. The continuous-wave (CW) pump scheme is no longer suitable at low repetition rates because of its relatively low amplification efficiency and reduced signal-to-noise ratio (SNR), as well as its harmful thermal effect. Recently, the pulsed pump scheme has been proposed and it has been experimentally demonstrated to overcome these drawbacks[2−9]. Furthermore, the transient response of an YDFA without signal injection has been numerically analyzed to guide the optimization of pump pulse duration[10,11]. However, all pump pulses in the aforementioned reports have relatively low pump power (less than hundreds of watts) and long pulse duration (tens to hundreds of microseconds). Although the useless pump energy and the harmful amplified spontaneous emission (ASE) between the signal intervals can be avoided using this low-power pulsed pump, the ASE that accompanies the output signal pulse has not been suppressed sufficiently, which will affect the subsequent amplification in a multi-stage amplifier and limit the SNR improvement. Pump parameters should be optimized further for some applications that require extremely high SNR.

In this letter, we report a theoretical study of a pulsed pumping YDFA. We propose a pulsed pump with kilowatt-level peak power and nanosecond-level duration and investigate its effect on transient dynamics and pulse amplification. Compared with a CW pump and a low-power pulsed pump, the high-power pulsed pump has proven more effective in improving the SNR and decreasing the output signal distortion. The study also discusses the pump parameters used to obtain the optimal SNR while maintaining the signal gain.

The schematic diagram of a pulsed pumping YDFA is presented in Fig. 1, which uses a large-mode-area (LMA) ytterbium-doped double-clad (YDDC) fiber to achieve a high energy output and suppress nonlinear effects. We adopted a forward pumping scheme to obtain output pulses with a high SNR[12]. To simplify the simulation, the pump pulse waveform is set as rectangular and the signal pulse as Gaussian. Meanwhile, the pump and the signal pulses operate at the same repetition rate.

Considering Yb^{3+} has a broad emission spectrum, we assume that the ASE within 100 nm centered at signal wavelength λ_s cannot be ignored. The ASE spectrum is divided into K channels, with an equal spacing $\Delta\lambda$ at central wavelength λ_k, $k = 1, 2, \cdots, K$. The spacing $\Delta\lambda$ is set equal to the signal bandwidth $\Delta\lambda_s$, which is 2 nm. The rate equations for the YDFA are given as[12]

$$\frac{\mathrm{d}N_2(z,t)}{\mathrm{d}t} = \frac{\Gamma_p\lambda_p}{hcA}[\sigma_a(\lambda_p)N_1(z,t) - \sigma_e(\lambda_p)N_2(z,t)] \cdot P_p(z,t) - \frac{N_2(z,t)}{\tau} + \frac{\Gamma}{hcA}\sum_{k=1}^{K} \cdot \lambda_k[\sigma_a(\lambda_k)N_1(z,t) - \sigma_e(\lambda_k)N_2(z,t)] \times [P^+(z,t,\lambda_k) + P^-(z,t,\lambda_k)], \quad (1)$$

$$N = N_1(z,t) + N_2(z,t), \quad (2)$$

$$\frac{\partial P_p(z,t)}{\partial z} + \frac{1}{\upsilon_p}\frac{\partial P_p(z,t)}{\partial t} = \Gamma_p[\sigma_e(\lambda_p)N_2(z,t) - \sigma_a(\lambda_p)N_1(z,t)]P_p(z,t) - \alpha P_p(z,t), \quad (3)$$

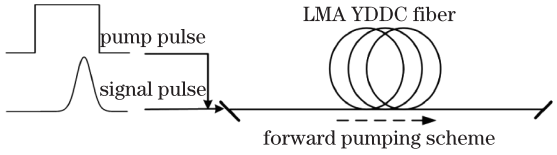

Fig. 1. Schematic diagram of a pulsed pumping YDFA.

$$\pm\frac{\partial P^{\pm}(z,t,\lambda_k)}{\partial z}+\frac{1}{v_{\rm p}}\frac{\partial P^{\pm}(z,t,\lambda_k)}{\partial t}=\Gamma_{\rm s}[\sigma_{\rm e}(\lambda_k)N_2(z,t)-\sigma_{\rm a}(\lambda_k)N_1(z,t)]P^{\pm}(z,t,\lambda_k)-\alpha P^{\pm}(z,t,\lambda_k)+2\sigma_{\rm e}(\lambda_k)N_2(z,t)\frac{hc^2}{\lambda_k^3}\Delta\lambda+S_{\rm R}P^{\mp}(z,t,\lambda_k), \quad (4)$$

where N is the concentration of Yb^{3+}; $N_1(z,t)$ and $N_2(z,t)$ are the ground and the upper level population densities, respectively; $P_{\rm p}(z,t)$ is the forward pump power; $P^{+}(z,t,\lambda_{\rm s})$ is the signal power when $k=s$; $P^{\pm}(z,t,\lambda_k)$ is the ASE power of each channel ($\pm$ corresponds to forward and backward directions). The constant c is the velocity of light in a vacuum; $\Gamma_{\rm p}$ and Γ are the power overlapping factors of the pump and signal (and ASE), respectively; $A=\pi(D_{\rm core}/2)^2$ is the doped area, where $D_{\rm core}$ is fiber core diameter; α is the fiber attenuation coefficient; $S_{\rm R}$ is the Rayleigh scattering coefficient; $\sigma_{\rm a}$ and $\sigma_{\rm e}$ are the absorption and emission cross sections of ytterbium ions; τ is the upper-level lifetime; $v_{\rm p}$ and v are the group velocity of the pump pulse and ASE (and signal), respectively. The chromatic dispersion effect is neglected in our simulation.

Considering that the fiber amplifier operates at a low-repetition rate, almost all of the remaining upper-level populations dissipate before the next pump pulse arrives after amplifying one signal pulse. Instead of including the effect of repetition rate, one amplification period is adequate for analysis because the amplification of adjacent signal pulses is independent. Based on this assumption, the initial conditions are

$$N_2(z,0)=0, \quad (5)$$

$$P_{\rm p}(z,0)=0,\quad P^{\pm}(z,0,\lambda_k)=0,\ (k=1,2,\cdots,K). \quad (6)$$

The boundary conditions are

$$P_{\rm p}(0,t)=P_{\rm p}(t),\quad P^{\pm}(0,t,\lambda_{\rm s})=P_{\rm in}(t), \quad (7)$$

$$P^{+}(0,t,\lambda_k)=0,\quad P^{-}(L,t,\lambda_k)=0,\quad (k=1,2,\cdots,K,\ \text{and}\ k\neq s). \quad (8)$$

where $P_{\rm p}(t)$ and $P_{\rm in}(t)$ are the input pump and signal pulse, respectively. The partial differential Eqs. (1) to (4) are solved using the time-dependent finite-difference method[13].

To analyze the amplification characteristics quantitatively, the stored energy, signal gain, and SNR are defined as

$$E_{\rm store}(t)=hv_{\rm s}A\int_0^L N_2(z,t){\rm d}z, \quad (9)$$

$${\rm Gain}=10\log\frac{\int_{-T/2}^{T/2}P^{+}(L,t,\lambda_{\rm s}){\rm d}t}{\int_{-T/2}^{T/2}P_{\rm in}(t){\rm d}t}, \quad (10)$$

$${\rm SNR}=10\log\frac{\int_{-T/2}^{T/2}P^{+}(L,t,\lambda_{\rm s}){\rm d}t}{\sum_{k=1(k\neq s)}^{K}\int_{-T/2}^{T/2}P^{+}(L,t,\lambda_k){\rm d}t}, \quad (11)$$

where L is the fiber length and T is the time window in which the output signal power is non-zero.

We have mainly discussed the contribution of the inner-pulse ASE to the output SNR because the inter-pulse ASE can be cut off.

The behavior of a pulsed pumping YDFA can be numerically analyzed based on the theoretical model above. The YDFA parameters are listed in Table 1[14]. The length of the amplifier is fixed at 5 m.

The energy stored and the ASE built-up prior to the arrival of the signal pulse is crucial to pulse amplification. Thus, we investigate transient dynamics of the YDFA without initial signal injection. The stored energy evolution and the output ASE under different pump power levels is plotted in Fig. 2. As shown in Fig. 2(a), with a relatively low power pump of 100 W, the stored energy increases linearly from the start of pumping, whereas the output ASE accumulates with a certain time delay. The backward ASE increases sooner and higher than the forward ASE because of the forward pump configuration[10]. The amplifier stabilizes with a sufficiently long pump time. Some differences become significant with greatly increasing the pump power up to the kilowatt level. As shown in Fig. 2 (b), using a 10-kW pump, the stored energy and the output ASE undergo the damped relaxation oscillation before approaching stability. The oscillating structure can be explained by the competition between the pumping process and the stimulated emission process, referring to the similar time behavior in a fiber laser[15]. Stability is achieved much sooner and the stored energy reaches a higher value in the first peak of oscillation because of the much higher pumping rate. However, the excessive upper-level population is quickly consumed by the high ASE. Compared with using a low-power pump, the amplifier is stable at almost the same stored energy but with a much higher ASE output using a high-power pump.

If the pump is cut off too early, the ASE is sufficiently suppressed but the amplification is limited. If the pump is cut off too late, the amplifier becomes stable and the ASE has already accumulated. Therefore, the pump should be terminated when the amplifier has just stored energy to reach a steady value in the pulsed pump scheme[10]. The time is shown by dash lines in Fig. 2. To achieve the same steady energy value of 4.2 mJ, the corresponding forward ASE is suppressed to 7.8 W under the 100-W pulsed pump, whereas the forward ASE is reduced further by half to 3.5 W under the 10-kW pulsed pump with much shorter pump duration.

Table 1. Parameters in the Simulation

A	4.91×10^{-10} m^2	N	6.00×10^{25} m^{-3}
$\lambda_{\rm p}$	915 nm	τ	0.84 ms
$\lambda_{\rm s}$	1 053 nm	α	3.00×10^{-3} m^{-1}
λ_1	1 002 nm	$\sigma_{\rm a}(\lambda_{\rm p})$	8.00×10^{-25} m^2
λ_K	1 100 nm	$\sigma_{\rm e}(\lambda_{\rm p})$	5.00×10^{-26} m^2
$\Delta\lambda$	2 nm	$\sigma_{\rm a}(\lambda_{\rm s})$	9.24×10^{-27} m^2
$\Gamma_{\rm p}$	0.01	$\sigma_{\rm e}(\lambda_{\rm s})$	3.59×10^{-25} m^2
Γ	0.85	$\sigma_{\rm a}(\lambda_k)$	see Ref. [14]
$S_{\rm R}$	1.20×10^{-7} m^{-1}	$\sigma_{\rm e}(\lambda_k)$	see Ref. [14]

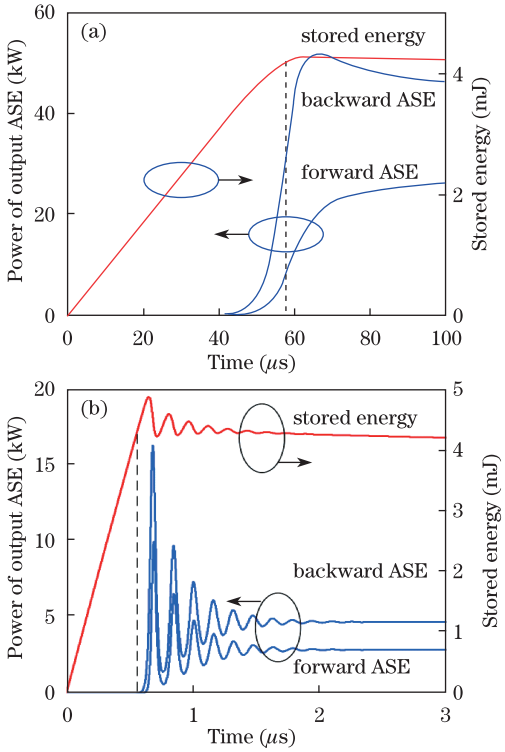

Fig. 2. (Color online) Evolution of the stored energy and the output ASE (a) with low pump power of 100 W and (b) with high pump power of 10 kW.

Continuing to increase the pump power causes the maximum stored energy to increase linearly and the corresponding pump time to decrease exponentially, as shown in Fig. 3. The steady energy value changes little with the variations in pump power, which can still be set to 4.2 mJ. Higher maximum stored energy allows the amplifer to reach the steady energy value much earlier than the ASE accumulates. The corresponding forward ASE can be further reduced using a pump with higher power, as depicted in Fig. 4. With a 50-kW pump power, the pump duration should be 118.5 ns, at which the forward ASE is 0.2 W, which is only 2.8% of that using a 100-W pump. A high-power pump pulse, with kilowatt-level pump power and nanosecond-level pulse duration, suppresses the ASE more efficiently without sacrificing the energy storage for high-energy amplification.

To analyze the pulse amplification, we consider an input signal which is a Gaussian pulse with peak power of 100 W and full-width at half-maximum (FWHM) of 10 ns. According to these experimental results[2−5], the input pulse should be injected at the end of the pump pulse for effective pump energy utilization. In our simulation, the center of the input signal is set 20 ns ahead of the trailing edge of the pump pulse (two times the input pulse FWHM) to ensure that the whole signal is amplified.

The evolution of the output signal and the output forward ASE under different pumping schemes is described in Fig. 5. A CW pump is included to analyze the improvement in the SNR using the high-power pulsed pump and the low-power pulsed pump. The horizontal axis shows the retarded time window that moves with the pulse at group velocity. The zero time corresponds to the center of the input pulse. Based on the amplifier parameters mentioned above, the stored energy of the amplifier reaches saturation using a 13-W CW pump, which provides an output pulse with a signal gain of 32.0 dB and a SNR of 46.5 dB. To facilitate comparison, the pump duration of the pulsed pump schemes is adjusted to achieve the same signal gain. The outputs using the low-power (100 W) pulsed pump and 53.9-μs pulse duration are almost the same as that using the CW pump, except for a slightly lower forward ASE. The output SNR is only improved by 1.9 dB to achieve the same signal gain. However, using the high-power (50 kW) pulsed with 122.3-ns pulse duration lowers the output signal distortion and allows the output forward ASE to accumulate slightly before the arrival of the signal. With the same signal gain, the output SNR is as high as 60.0 dB, which is 13.5 dB higher than that using the CW pump and 11.6 dB higher than that using the low-power pulsed pump. These results indicate that the high-power pulsed pumping YDFA yields a high-energy output signal pulse with a high SNR by avoiding the interpulse ASE and effectively suppressing the inner-pulse ASE. By contrast, the improvement in the SNR is limited using the low-power pulsed pump.

We analyzed the evolution of the stored energy under different pumping schemes to understand better the pulse amplification dynamics (Fig. 6). The stored energy using the low-power pulsed pump exhibits similar variations to that using the CW pump. However, the stored energy in the high-power pulsed pumping amplifier still undergoes the rapid growth before signal injection. During this time, the ASE is efficiently suppressed because of the relatively low upper-level population, which

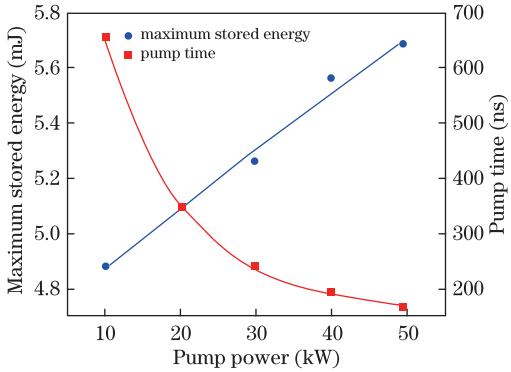

Fig. 3. Maximum stored energy and the corresponding pump time under different pump power levels.

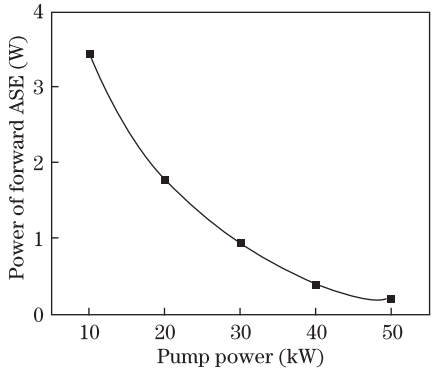

Fig. 4. Forward ASE at a stored energy of 4.2 mJ under different pump power levels.

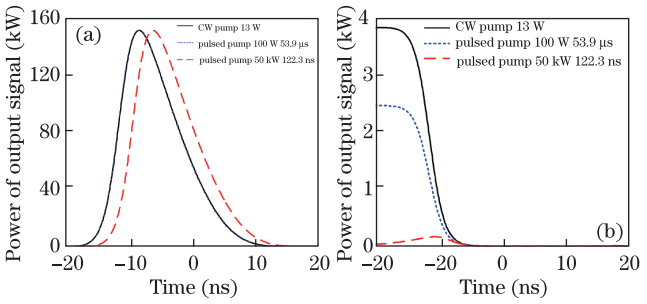

Fig. 5. Evolutions of (a) the output signal pulse and (b) the output forward ASE under different pump schemes.

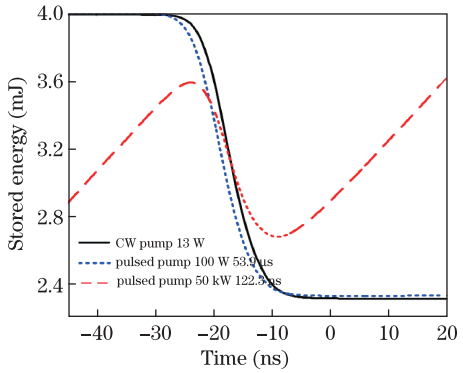

Fig. 6. Evolution of the stored energy under different pump schemes.

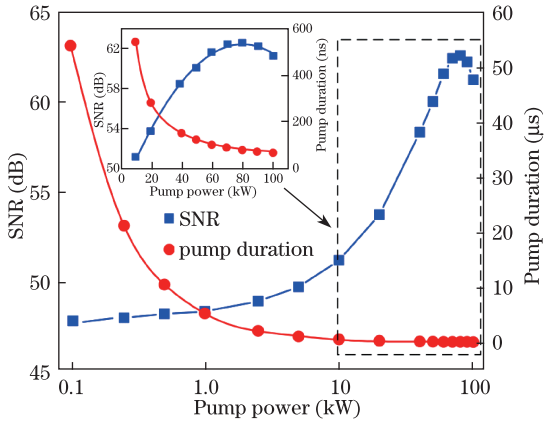

Fig. 7. Variations in output SNR and required pump duration with pump power at a fixed signal gain of 32.0 dB.

improves the output SNR. The amplifer consumes less stored energy to achieve the same signal gain under the high-power pulsed pump. The high amplification efficiency and high recovery rate of the stored energy reduces the difference between the signal gain of the leading edge and that of the trailing edge, which decreases output pulse distortion (as mentioned above).

Figure 7 shows the variations in output SNR and required pump duration with pump power at a fixed signal gain of 32.0 dB. The pump duration needed to maintain the same signal gain is much shorter at a higher pump power. The high-power pulsed pump with kilowatt-level peak power and nanosecond-level duration produces output signal with sufficiently improved SNR. Using an 80-kW pulsed pump and an 82.5-ns pulse duration, the amplifier achieves an optimal output SNR of 62.3 dB.

In conclusion, the dynamic characteristics of a pulsed pumping YDFA are investigated in detail. We analyze the accumulation of stored energy and ASE in a fiber amplifier using different pump power levels. The results show that a higher-power pump pulse, with kilowatt-level pump power and nanosecond-level pulse duration, suppresses the ASE more efficiently without sacrificing the energy storage. Then, we compare the outputs of amplifier under different pump schemes. In our simulation, a signal gain of 32.0 dB (the same with that using a 13-W CW pump), the 50-kW pulsed pump with 122.3-ns pulse duration improves the SNR by 13.5 dB, whereas the 100-W pulsed pump with 53.9-μs pulse duration only improves the SNR by 1.9 dB. The high-power pulsed pump with kilowatt-level peak power and nanosecond-level duration greatly improves the SNR and reduces output signal distortion. By adjusting the pump parameters, the amplifier can achieve an optimal SNR of 62.6 dB while maintaining the signal gain. We believe that high-power pulsed pumps are very suitable for high-energy nanosecond pulse amplification, which has a high SNR requirement. Furthermore, these pump pulses can be achieved using a Q-switching fiber laser[16].

References

1. P. Jiang, D. Yang, Y. Wang, T. Chen, B. Wu, and Y. Shen, Laser Phys. Lett. **6,** 384 (2009).
2. C. Ye, P. Yan, M. Gong, and M. Lei, Chin. Opt. Lett. **3,** 249 (2005).
3. M. D. Mermelstein, in *Proceedings of Optical Amplifiers and Their Applications/Coherent Optical Technologies and Applications* OMC2 (2006).
4. X. Huang, B. Guo, W. Yang, G. Chen, X. Gong, Y. Kong, D. Li, X. Li, Z. Sui, M. Li, and J. Wang, Chin. Opt. Lett. **7,** 712 (2009).
5. Y. Kong, Q. Liu, C. Deng, F. Tian, and X. Huang, J. Modern Opt. **56,** 597 (2009).
6. W. Cheng, H. Zhang, M. Liu, C. Zheng, P. Yan, and M. Gong, J. Opt. **13,** 085204 (2011).
7. P. Wan, J. Liu, L. Yang, and F. Amzajerdian, Opt. Express **19,** 18067 (2011).
8. H. Kalaycioglu, K. Eken, and F. Ö Ilday, Opt. Lett. **36,** 3383 (2011).
9. C. Zheng, H. Zhang, P. Yan, and M. Gong, Opt. Laser Technol. **49,** 284 (2013).
10. T. Wei, J. Li, and J. Zhu, Chin. Opt. Lett. **10**, 040605 (2012).
11. W. Zhang, J. Ning, and B. Chen, Adv. Mater. Res. **403,** 2508 (2012).
12. W. Yong and P. Hong, J. Lightwave Technol. **21,** 2262 (2003).
13. R. LeVeque, *Finite Difference Methods for Ordinary and Partial Differential Equations: Steady-State and Time-dependent Problems* (Society for Industrial and Applied Mathematics, Philadelphia, 2007).
14. R. Paschotta, J. Nilsson, A. C. Tropper, and D. C. Hanna, IEEE J. Quantum Electron. **33,** 1049 (1997).
15. O. Svelto, *Principles of lasers* (Springer, Berlin, 2009).
16. J. Boullet, R. Dubrasquet, C. Médina, R. Bello-Doua, N. Traynor, and E. Cormier, Opt. Lett. **35,** 1650 (2010).